

Influence of Staging on Re-Entry Trajectory Characteristics

DUANE E. RANDALL*

Sandia Laboratories, Albuquerque, N. Mex.

Nomenclature

a	= acceleration
B	= ballistic coefficient, weight/(drag coefficient) (reference area)
D	= constant in heating rate expression, Eq. (21)
g	= acceleration of gravity
K	= (exponential approximation for $\rho_{y=0}/\rho_0$)
n	= exponent in heating rate expression, Eq. (21)
\dot{q}_0	= cold-wall, stagnation-point heating rate
\mathbf{V}	= velocity
y	= altitude
β	= constant in density approximation, $\rho \simeq K\rho_0 e^{-\beta y}$
γ	= flight path angle referenced to the local horizon
ρ	= density
ρ_0	= U.S. Standard Atmosphere sea level density
ξ, ζ, ψ	= functions defined by Eqs. (2, 12, and 17), respectively

Subscripts

I	= initial point of atmospheric reentry
E, P	= ejected body and parent body, respectively
sep	= at separation altitude

Introduction

NUMEROUS situations exist in which two joined bodies re-enter the Earth's atmosphere and at some point along the trajectory separate; e.g., a radioisotopic, thermoelectric generator may separate from a spacecraft, or a fuel capsule may separate from a generator. The objective of this Note is to define the influence of the parent body and the separation point on the aerodynamic loading and the heating experienced by the ejected body.

Aerodynamic Analysis

Allen¹ has developed an analytic solution to the equations of motion for a re-entry body by neglecting the gravity term and by assuming that the ballistic coefficient B and the flight path angle γ are constants. This technique provides a good approximation of the actual motion unless γ_I is very small or the velocity decreases to a point where it influences B . For usual re-entry configurations the deceleration and heating pulses occur prior to any influence of V on B . Under these conditions, the differential equation of motion has a solution of the form

$$\ln V = -\xi + \text{const} \quad (1)$$

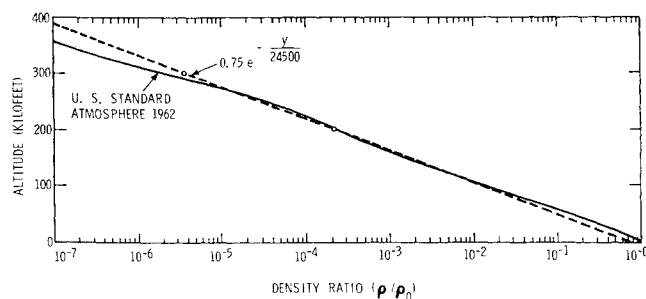


Fig. 1 Comparison of exponential and 1962 U.S. Standard atmosphere density ratios.

Received September 5, 1969; revision received December 15, 1969.

* Staff Member, Reentry & Space Sciences Division. Associate Fellow AIAA.

where

$$\xi \equiv gK\rho_0 e^{-\beta y}/2\beta B \sin \gamma \quad (2)$$

With $K = 0.75$ and $\beta = \frac{1}{24500}$, the exponential approximation for density agrees with the 1962 U.S. Standard Atmosphere² density within $\pm 15\%$ for $100,000 < y < 260,000$ ft (Fig. 1), which includes the region of the re-entry deceleration and heating pulses. For a single stage trajectory, the boundary condition defining the integration constant, as formulated by Allen, is $V = V_I$ at $y = 456,000$ ft (75 naut miles). The exponential term becomes vanishingly small and is neglected at this altitude. Thus,

$$V = V_I e^{-\xi} \quad (3)$$

and the expressions for deceleration, maximum deceleration, and altitude of peak deceleration are, respectively,

$$-a = V_I^2 (gK\rho_0/2B) e^{-\beta y - 2\xi} \quad (4)$$

$$-a_{\max} = V_I^2 (\beta \sin \gamma)/2e \quad (5)$$

$$y_{a_{\max}} = \beta^{-1} \ln(gK\rho_0/\beta B \sin \gamma) \quad (6)$$

These same solutions are applicable to the initial section of a staged re-entry trajectory.

Let us consider a two-body system re-entering in unison until separation occurs instantaneously at altitude y_{sep} . The parent body experiences no discontinuity in \mathbf{V}_P or γ_P . The ejected body is permitted a step change from γ_P to γ_E at separation, but $|\mathbf{V}|$ remains the same; i.e., $|\mathbf{V}_E| \equiv |\mathbf{V}_P|$ is a constraint for the model. This model permits one to integrate the equation of motion in two steps to achieve a solution for each section of the trajectory. Figure 2 illustrates the model for two cases: $\gamma_E > \gamma_P$, and $\gamma_E < \gamma_P$. At separation, $\mathbf{V}_E = \mathbf{V}_P + \Delta\mathbf{V}$. Resolving \mathbf{V}_E and \mathbf{V}_P into their components and introducing the constant speed constraint, $|\mathbf{V}_E| = |\mathbf{V}_P|$, one sees that

$$\gamma_E - \gamma_P = \pm 2 \sin^{-1}(\Delta\mathbf{V}/2V) \quad (7)$$

For small $\Delta\mathbf{V}/V$, $\Delta\mathbf{V}/V \approx \sin(\Delta\mathbf{V}/V)$, and

$$\gamma_E - \gamma_P = \pm \Delta\mathbf{V}/V (\text{rad}) = \pm (180/\pi)(\Delta\mathbf{V}/V) (\text{deg}) \quad (8)$$

For Sect. II (see Fig. 2) of the trajectory involving the ejected body, the same differential equation and the solution [Eq. (1)] are applicable. However, the integration constant is now evaluated for the boundary conditions $y = y_{\text{sep}}$, $\mathbf{V} = \mathbf{V}_{\text{sep}}$, so that:

$$\text{integration const} = \ln \mathbf{V}_{\text{sep}} + \xi_{E, \text{sep}} \quad (9)$$

where $\xi_{E, \text{sep}}$ is evaluated for $y = y_{\text{sep}}$. But since $\mathbf{V}_{\text{sep}} = \mathbf{V}_P$ ($= \mathbf{V}_E$ immediately prior to separation), \mathbf{V}_{sep} may also be defined in terms of trajectory section I parameters as

$$\mathbf{V}_{\text{sep}} = \mathbf{V}_I e^{-\xi_{P, \text{sep}}} \quad (10)$$

and hence,

$$\mathbf{V}_E = \mathbf{V}_I e^{\xi_E - \xi_E} \quad (11)$$

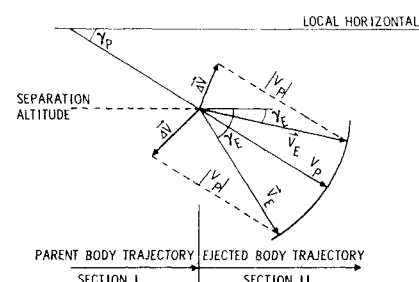


Fig. 2 Model for two-body system.

where

$$\zeta \equiv \xi_{E,sep} - \xi_{P,sep} \quad (12)$$

$$-a_E = V_I^2 (gK\rho_0/2B_E) e^{2\zeta - \beta y - 2\xi_E} \quad (13)$$

$$-a_{E,max} = V_I^2 [(\beta \sin \gamma_E)/2e] e^{2\zeta} \quad (14)$$

$$y_{E,a_{max}} = \beta^{-1} \ln(gK\rho_0/\beta B_E \sin \gamma_E) \quad (15)$$

Note that we are assuming, for convenience, that a single atmosphere approximation (K and β) spans both sections of the trajectory. A further simplification is obtained by expressing y_{sep} in terms of the altitude of $\dot{V}_{E,max}$. Thus,

$$y_{sep} = y_{E,a_{max}} + \Delta y_{sep} \quad (16)$$

where $y_{E,a_{max}}$ is given by (15). Incorporation of these modifications in Eqs. (11 and 13-15) is done simply by replacing ζ in these equations by

$$\psi \equiv \frac{1}{2} [1 - \{(B_E \sin \gamma_E)/(B_P \sin \gamma_P)\}] e^{-\beta \Delta y_{sep}} \quad (17)$$

The influence of staging on the ejected body is conveniently defined in terms of the characteristics that the same body would experience on a nonstaged reentry trajectory. Dividing the staged trajectory velocity and decelerations (expressed in the new equations containing e^ψ or $e^{2\psi}$) by the nonstaged values of the same parameters defined by Eqs. (3-5), we obtain

$$V_E/V = e^\psi \quad (18)$$

$$a_E/a = e^{2\psi} \quad (19)$$

Thus,

$$a_E/a = (V_E/V)^2 \quad (20)$$

The ratio of the maximum decelerations is also given by (19) or (20), since the ratio is independent of altitude following separation.

Aeroheating Analysis

A reference configuration commonly used for evaluating the reentry trajectory heating rate is a 1-ft-radius hemisphere, for which the cold-wall, stagnation-point heating rate may be expressed as^{1,3,4}

$$\dot{q}_0 = D\rho^{1/2}V^n \quad (21)$$

On substituting the density approximation and the velocity from Eq. (3), the \dot{q}_0 experienced on Sec. I of the re-entry trajectory is

$$\dot{q}_0 = DV_I^n (K\rho_0)^{1/2} e^{-\beta y/2 - n\xi} \quad (22)$$

Then

$$\dot{q}_{0,max} = DV_I^n [\langle \beta B \sin \gamma \rangle / nge]^{1/2} \quad (23)$$

occurs at

$$y_{max \dot{q}_0} = \beta^{-1} \ln(ngK\rho_0/\beta B \sin \gamma) \quad (24)$$

By conducting a treatment similar to that just carried out,

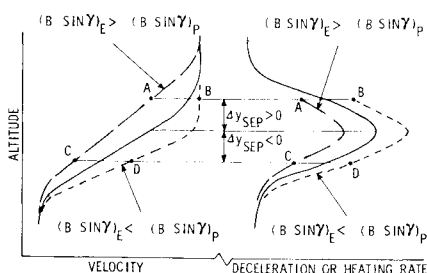


Fig. 3 Typical re-entry behavior.

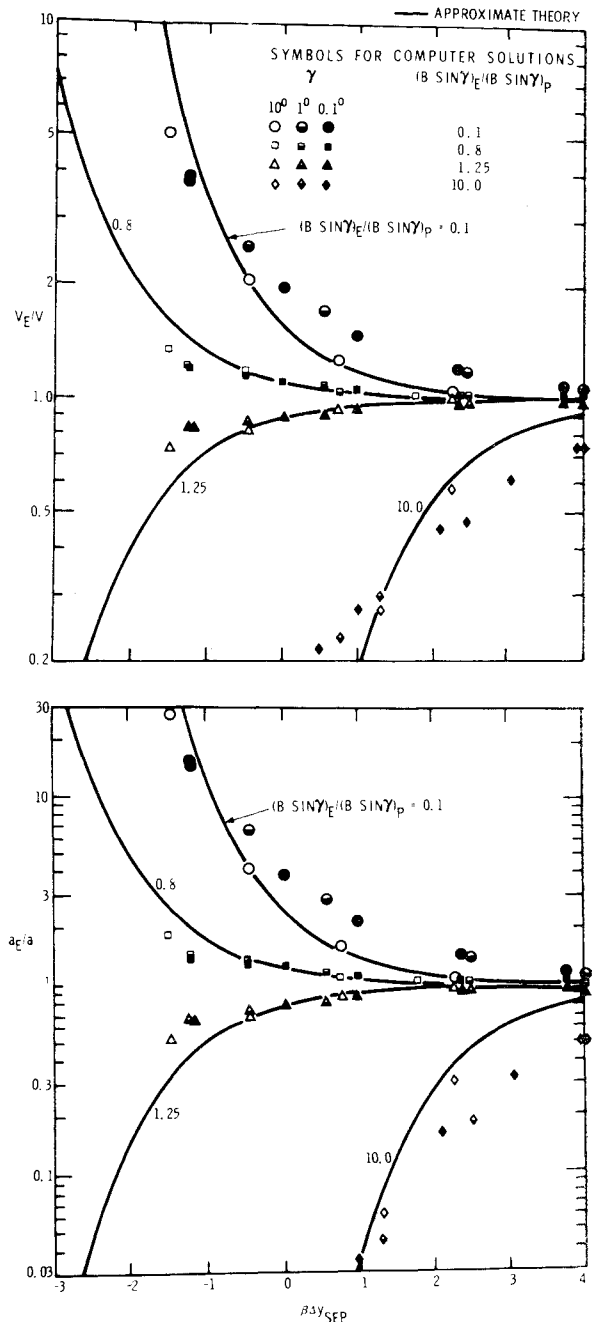


Fig. 4 Comparison of velocity and deceleration ratios.

the ratio of the heating rate experienced by an ejected body on Sec. II of its re-entry trajectory to the heating rate experienced by a similar body (same $B \sin \gamma$) on a nonstaged reentry trajectory is

$$\dot{q}_{0E}/\dot{q}_0 = e^{\psi'} \quad (25)$$

where ψ' is given by (17), except that Δy_{sep} is replaced by $\Delta y'_{sep}$, the latter being measured from $y_{max \dot{q}_0}$. Thus, \dot{q}_{0E}/\dot{q}_0 is mathematically equivalent to V_E/V [Eq. (18)] if Δy_{sep} is measured from the altitude of peak heating rather than the altitude of peak deceleration.

Discussion and Comparisons with Numerical Results

The re-entry trajectory characteristics expressed by V , a , and \dot{q}_0 have been defined for a body which is ejected or separated from a parent body at an arbitrary point along the reentry trajectory. An analysis of Eqs. (18, 19, and 25) affords the following observations for three cases:

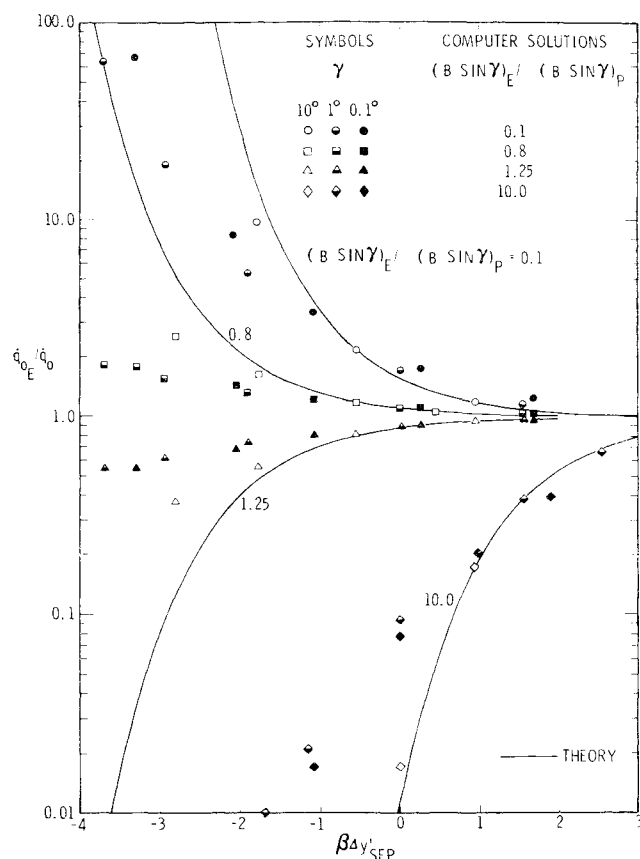


Fig. 5 Comparison of heating rate ratios.

Case 1: If $B_E \sin \gamma_E = B_P \sin \gamma_P$, then \mathbf{V}_E , \mathbf{a}_E , and \dot{q}_{0E} are the same as would be experienced on a nonstaged trajectory for the same $B \sin \gamma$.

Case 2: If $B_E \sin \gamma_E > B_P \sin \gamma_P$, then \mathbf{V}_E , \mathbf{a}_E , and \dot{q}_{0E} are less than would be experienced on a nonstaged trajectory for the same $B \sin \gamma$ ($= B_E \sin \gamma_E$).

Case 3: If $B_E \sin \gamma_E < B_P \sin \gamma_P$, then \mathbf{V}_E , \mathbf{a}_E , and \dot{q}_{0E} are greater than would be experienced on a nonstaged trajectory for the same $B \sin \gamma$ ($= B_E \sin \gamma_E$).

These relations are illustrated graphically in Fig. 3 for typical re-entry behavior. The solid lines represent the nonstaged trajectory for $B \sin \gamma = B_E \sin \gamma_E$ (case 1). The long-dashed curves represent case 2; the short dashed curves, case 3. Points A and B, for cases 2 and 3, respectively, represent situations where separation occurs before the altitude of peak deceleration or peak heating rate for the ejected body is reached; i.e., $\mathbf{a}_{E\max}$ and $\dot{q}_{0E\max}$ are experienced following release. Points C and D represent the similar situations where y_{sep} is below the computed altitude of peak deceleration or peak heating rate for the ejected body. In this event, \mathbf{a}_E and \dot{q}_{0E} decrease monotonically with time following release.

Figures 4 and 5 compare these theoretical approximations (the curves) with solutions (points for y_{sep}) provided by a digital program⁵ (which numerically integrates the complete equations of motion) for $V_I = 24,000$ fps and for $(B \sin \gamma)_E / (B \sin \gamma)_P = 10, 1.25, 0.8$, and 0.1 . Separation altitudes investigated spanned the range from above the peak heating rate to below peak deceleration. For each value of $(B \sin \gamma)_E / (B \sin \gamma)_P$, computer trajectory solutions were calculated for γ_I 's of 10° , 1° and 0.1° to cover the range from steep ballistic or launch abort re-entry to shallow orbital decay reentry. Whereas the approximate theory indicates that the \mathbf{V} , \mathbf{a} and \dot{q}_0 ratios are constant following separation, the computer solutions indicate that the ratios tend to approach unity with increasing time following separation. The approximate theory does, however, provide a good

correlation of the ratios at y_{sep} , and it quite adequately indicates the influences of the various parameters involved. It is apparent that the influence of the staging process on the velocity, deceleration, and stagnation point heating rate increases as separation is delayed along the trajectory (i.e., as Δy_{sep} decreases to negative values) or as the disparity in $B \sin \gamma$ values for the ejected and parent bodies increases.

References

- Allen, H. J. and Eggers, A. J., Jr., "A Study of the Motion and Aerodynamic Heating of Ballistic Missiles Entering the Earth's Atmosphere at High Supersonic Speeds," Rept. 1381, 1958, NACA.
- U.S. Standard Atmosphere, 1962, Superintendent of Documents, U.S. Government Printing Office, Washington 25, D.C.
- Kemp, N. H. and Riddell, F. R., "Heat Transfer to Satellite Vehicles Re-entering the Atmosphere," *Jet Propulsion*, Vol. 27, No. 2, Feb. 1957, pp. 132-137.
- Detra, R. W., Kemp, N. H., and Riddell, F. R., "Addendum to Heat Transfer to Satellite Vehicles Re-entering the Atmosphere," *Jet Propulsion*, Vol. 27, No. 12, Dec. 1957, pp. 1256-1257.
- Allensworth, J. A. F., "The TTA Generalized Rigid Body Trajectory Program for Digital Computer," SC-DR-65-511, Aug. 1966, Sandia Labs., Albuquerque, N. Mex.

Radiation Heat Transfer Around the Interior of a Long Cylinder

JOHN D. GRAHAM*

Spar Aerospace Products, Mallon, Ontario, Canada

Nomenclature

- A, A_1 = area elements on cylinder surface
- B, F, H = $B(\theta), F(\theta), H(\theta)$, Eqs. (6, and 8), respectively
- b, b_1 = one half length of longitudinal area elements
- C, D = solution constants, see Eq. (11)
- E = emissive power
- l_1 = see Ref. 3
- q_0 = net heat loss at position zero
- r = cylinder radius
- T_θ = temperature at position θ
- ϵ = interior surface emissivity to (and absorptivity for) infrared radiation
- θ = position around cylinder (see Fig. 1)
- σ = Stefan-Boltzmann constant
- ϕ, ϕ_1 = see Ref. 3

Introduction

THERE is presented the derivation of a simple expression for the radiation heat transfer around the interior of a long cylinder in terms of the emissivity ϵ of the surface. It is assumed that ϵ is constant over the entire surface and that all reflections are diffuse. Also, the temperature distribution is assumed independent of length.

One of the immediate applications for this result is in determining radiant heat transfer in STEMs.¹ Often in the thermal analysis of conventional STEMs the radiant heat transfer can be neglected, as it is small compared to conduction around the metallic cross section. However, some recent STEM concepts² have an overlapping type contact across which the conduction is poor, thus necessitating the consideration of radiation heat transfer.

Specifically we will find an expression for $B(\theta)$ which is the proportion of radiation emitted from a longitudinal area element at position θ on the cylinder interior (Fig. 1) which,

Received July 23, 1969; revision received December 22, 1969. The support for this work was provided in part by D.I.R. Grant 5540/33 from the Defense Research Board of Canada.

* Head, Systems Analysis. Member AIAA.